

RESEARCH ARTICLE

Application of 2D-DIGE to formalin-fixed diseased tissue samples from hospital repositories: Results from four case studies

Alessandro Tanca¹, Salvatore Pisanu¹, Grazia Biosa¹, Daniela Pagnozzi¹, Elisabetta Antuofermo², Giovanni P. Burrai², Vincenzo Canzonieri³, Paolo Cossu-Rocca⁴, Valli De Re³, Albino Eccher⁵, Giuseppe Fanciulli⁴, Stefano Rocca², Sergio Uzzau^{1,6} and Maria Filippa Addis¹

¹ Porto Conte Ricerche Srl, Tramariglio, Alghero, Italy

² Dipartimento di Medicina Veterinaria, Università di Sassari, Sassari, Italy

³ Centro di Riferimento Oncologico, IRCCS National Cancer Institute, Aviano, Italy

⁴ Dipartimento di Medicina Clinica e Sperimentale, Università di Sassari, Sassari, Italy

⁵ Dipartimento di Patologia e Diagnostica, Università di Verona, Verona, Italy

⁶ Dipartimento di Scienze Biomediche, Università di Sassari, Sassari, Italy

Purpose: In the recent past, the potential suitability of fixed samples to 2D-DIGE studies has been demonstrated on model tissues, but not on “real-world” archival tissues. Therefore, this study was aimed to assess the quality of the results delivered by 2D-DIGE on samples retrieved from hospital tissue repositories.

Experimental design: Diseased and normal tissue samples (namely, human gastric adenocarcinoma and normal gastric tissue, human lung neuroendocrine tumors, canine mammary tubulo-papillary carcinoma and normal mammary tissue, sheep liver with cloudy swelling degeneration and normal liver tissue) were retrieved from human and veterinary biorepositories and subjected to full-length protein extraction, cyanine labeling, 2D-DIGE separation, image analysis, MS analysis, and protein identification.

Results: Archival samples could be successfully subjected to 2D-DIGE, providing maps of satisfactory resolution, although with varying pattern complexity (possibly influenced by pre-analytical variables). Moreover, differentially expressed protein identities were consistent with the disease biology.

Conclusions and clinical relevance: 2D-DIGE can support biomarker discovery and validation studies on large sample cohorts. In fact, although some information complexity is lost when compared to fresh-frozen tissues, their vast availability and the associated patient information can considerably boost studies suffering limited sample availability or involving long-distance exchange of samples.

Keywords:

Canine mammary tumor / FFPE / Gastric adenocarcinoma / Gel-based proteomics / Lung neuroendocrine tumor



Additional supporting information may be found in the online version of this article at the publisher's web-site

Correspondence: Dr. Maria Filippa Addis, Porto Conte Ricerche Srl, S.P. 55 Porto Conte/Capo Caccia Km 8.400, Tramariglio, 07041 Alghero (SS), Italy

E-mail: addis@portocontericerche.it

Fax: +39-079-998-567

Abbreviations: BVA, biological variation analysis; DIA, differential in-gel analysis; FFPE, formalin-fixed paraffin-embedded; SCLC, small cell lung carcinoma; TC, typical carcinoid

1 Introduction

Although believed to be unsuitable to proteomic investigations until less than a decade ago, fixed tissues are increasingly delivering meaningful results and information in terms of disease biology and biomarker discovery. Numerous

Colour Online: See the article online to view Fig. 2 in colour.

Received: June 8, 2012

Revised: August 1, 2012

Accepted: September 28, 2012

research groups have contributed to this progress, leading to the development of progressively more performing extraction methods. These have relied mainly on two strategies: tryptic digestion of the fixed tissue matrix and extraction of full-length proteins. The analytical methods applied to peptides and proteins extracted from fixed tissues have spanned from gel-free to gel-based applications [1–5]. The latter, however, have been less explored, likely because of the need to release proteins from the entangled, cross-linked matrix created by the action of formalin on biological molecules, in order to make them suitable to electrophoretic separation. Nevertheless, the suitability of 2D-PAGE and 2D-DIGE to analysis of fixed samples has been demonstrated on model tissues, providing the proof-of-principle that these techniques can be applied with successful results [6–8]. Basically, the strategy applied in order to extract full-length proteins suitable to gel-based proteomics uses heat in combination with detergents and reducing agents, building on the seminal antigen retrieval technique devised by Shi and co-workers [9]. Here, heat and chemicals are believed to act by releasing proteins with a combination of factors, including “reversal” of cross-links introduced by formaldehyde among biological molecules, and disruption of their intermolecular interactions by prolonged exposure to extreme chemical conditions. However, the exact chemical events taking place in biological tissues during “retrieval” are yet to be completely understood [10].

Differential proteomic studies are gradually shifting from gel-based to shotgun approaches, which require sophisticated MS instrumentation and advanced data processing capabilities. Nevertheless, 2D-PAGE remains one of the workhorses of differential proteomics, mainly because of its ability to deliver results in a readily accessible, relatively inexpensive way, providing information on the global pattern of protein expression under conditions enabling the quantitative and qualitative study of all proteins in relation to each other [11]. In addition, 2D-PAGE enables to focus on the differences among samples without the need of analyzing the entire protein repertoire with more lengthy and complicated quantitative proteomics approaches, and the ability to easily visualize protein isoforms differing either in charge or molecular weight provides added informational value. However, in spite of its numerous advantages, classical 2D-PAGE still suffers several limitations, including poor reproducibility, low sensitivity, and narrow linear dynamic ranges [12]. Although sensitivity and linear dynamic range can be considerably increased with the adoption of fluorescent stains and powerful imaging instrumentation, the more critical issue remains reproducibility. In fact, experience and manual skill are required for limiting variability across gels, which can be considerably reduced by experienced operators but cannot be completely eliminated. Intergel, interoperator, and interlaboratory variability are in fact always an issue. Fluorescent 2D-DIGE offers a significant improvement in this respect, enabling the normalization of most of the technical variability in 2D-PAGE, together with a significant increase in sensi-

tivity and linear dynamic range due to the use of fluorescent dyes [13–15].

The applicability of 2D-DIGE to proteins extracted from fixed tissues is not a trivial task, since the limitations posed by chemical modification on protein separation add up to the need of unmodified lysine residues available for CyDye labeling. Nevertheless, the ability to successfully label and separate “retrieved” proteins has been recently demonstrated by our group using two model tissues, muscle and liver [8]. When starting from intact tissues and applying optimized fixation protocols, the results delivered by these proteins can be considered satisfactory. However, the transition from model samples to “real-world” tissues can be tricky. In fact, the tissue repositories in human and veterinary pathology departments have been generated along the years, often with variable fixation timings and protocols. Samples stored in these archives can span from blocks resulting from an extremely stringent and consistent procedure (use of reproducible tissue block sizes, consistent fixative amount and quality, defined fixation timing, and paraffin embedding) to large tissue pieces which have been left in formalin for years. Also, the tissue sample can be either collected bioptically and immediately fixed, with optimal results, or be the result of an autoptic or necroscopic procedure with deriving autolysis and tissue deterioration occurred before fixation.

In order to assess the performance of 2D-DIGE on these “real-world” samples, in this study, four different and heterogeneous hospital tissue repositories were exploited. Both human and veterinary sample repositories were chosen for the study in order to account for different conditions of collection (biopsy and necroscopy), fixation and storage times (shorter versus longer), and to include diverse disease types and tissue sources. In addition, human and animal tissues were included in this study with the aim of evaluating organisms and diseases for which complete proteomic databases were not readily available. Human, dog, and sheep samples with different histology and anatomical localizations were selected, subjected to optimized protein extraction, and analyzed by 2D-DIGE. Results were then evaluated in terms of quality of the protein separation, profile complexity, suitability to differential image analysis, and ability to deliver meaningful results in terms of disease biology.

2 Materials and methods

2.1 Tissue samples

Twelve formalin-fixed paraffin-embedded (FFPE) tissue specimens were retrieved from four different sample repositories located in Italy, including three Departments of Human Pathology and one of Veterinary Pathology. Clinical and laboratory features of the samples used in this study are listed in Table 1. Human and dog samples had been obtained as a result of bioptic procedures, while sheep samples had been collected at necroscopy within the day of slaughter. Shortly

Table 1. List of samples used in this study

Sample no.	Tissue repository	Taxonomy	Tissue	Diagnosis	Collection type	Time from collection to fixation (hours)	Fixation time (hours)	Storage time (months)
1A	Aviano—CRO Hospital	Human	Stomach	Adenocarcinoma	Surgical biopsy	1	36–48	15
1B	Aviano—CRO Hospital	Human	Stomach	Normal adjacent tissue (control)	Surgical biopsy	1	36–48	15
2A	Aviano—CRO Hospital	Human	Stomach	Adenocarcinoma	Surgical biopsy	1	36–48	19
2B	Aviano—CRO Hospital	Human	Stomach	Normal adjacent tissue (control)	Surgical biopsy	1	36–48	19
3	Verona—University Hospital	Human	Lung	Typical carcinoid	Surgical biopsy	1	36–48	6
4	Sassari—University Hospital	Human	Lung	Small cell lung carcinoma	Surgical biopsy	1	36–48	30
5	Sassari—Veterinary Dept	Dog	Mammary gland	Tubulo-papillary carcinoma	Surgical biopsy	1	48–56	22
6	Sassari—Veterinary Dept	Dog	Mammary gland	Tubulo-papillary carcinoma	Surgical biopsy	1	48–56	35
7	Sassari—Veterinary Dept	Dog	Mammary gland	Normal tissue (control)	Surgical biopsy	1	48–56	8
8	Sassari—Veterinary Dept	Dog	Mammary gland	Normal tissue (control)	Surgical biopsy	1	48–56	11
9	Sassari—Veterinary Dept	Sheep	Liver	Cloudy swelling	Necroscopy (at slaughter)	3	48–56	30
10	Sassari—Veterinary Dept	Sheep	Liver	Normal tissue (control)	Necroscopy (at slaughter)	3	48–56	30

after collection, all human and animal tissues had been fixed in 10% neutral buffered formalin at room temperature (20–25°C) for 36–48 h and 48–56 h, respectively, dehydrated and embedded in paraffin (FFPE), and then stored at room temperature (20–25°C). At the time of diagnosis, samples had been subjected to sectioning, staining with hematoxylin and eosin, histological examination and/or immunohistochemistry assessment, and classification according to the specific disease guidelines. In all cases, the use of historical fixed material for research purposes had been authorized by the local Ethical Committees.

2.2 Sample preparation

Ten serial, 5 µm thick, FFPE tissue sections were obtained from each tissue specimen using a microtome, and then subjected to deparaffinization, rehydration, and high-temperature protein extraction (in 20 mM Tris HCl, pH 8.8, 2% SDS, 200 mM DTT extraction buffer), according to an established procedure [16]. Protein extracts were precipitated

with the 2D Clean-Up Kit (GE Healthcare, Little Chalfont, UK), resuspended at a concentration of 1–5 mg/mL in a buffer composed by urea (7 M), thiourea (2 M), CHAPS (4%), and Tris-HCl (10 mM, pH 8.8), quantified using the EZQ Protein Quantification Kit (Molecular Probes, Eugene, OR, USA), and stored at –20°C until proteomic analysis.

2.3 2D-DIGE analysis

Protein extracts (50 µg per sample) were labeled with CyDyes DIGE Fluors (GE Healthcare), according to the minimal labeling protocol provided by the manufacturer, and properly combined as summarized in Table 2. IPG buffer corresponding to the desired pH range was added to a 1% final concentration, and DeStreak Rehydration Solution (GE Healthcare) was added to a total volume of 450 µL. Twenty-four centimeters IPG strips (GE Healthcare) were passively rehydrated for at least 12 h. IEF was carried out on an Ettan IPGphor 3 (GE Healthcare) for a total of ~90 000 Vh. After focusing, strips were equilibrated as described in [6] and subjected

Table 2. Design of 2D-DIGE experiments

Gel no.	pH range	Cy2	Cy3	Cy5
A1	3–11		Sample 1A	Sample 1B
A2	3–11		Sample 2B	Sample 2A
B	3–11		Sample 4	Sample 3
C1	4–7	Pool of samples 5–6–7–8	Sample 7	Sample 5
C2	4–7	Pool of samples 5–6–7–8	Sample 6	Sample 8
D	3–11		Sample 10	Sample 9

to SDS-PAGE in 10–18% gradient polyacrylamide 24 cm × 20 cm gels on an Ettan DALTtwelve system (GE Healthcare), following the manufacturer's instructions. Gel image acquisition was performed on a Typhoon Trio+ laser scanner (GE Healthcare) at 100 μm of resolution. The scanned gel images were then transferred to the ImageQuant software (version 5.2, GE Healthcare). After cropping, images were exported to PDQuest Advanced software (version 8.0, Bio-Rad, Hercules, CA, USA) in order to enumerate the total number of spots detected in each gel, by performing background subtraction and spot detection.

Finally, images were imported into the DeCyder software (version 7.0, GE Healthcare) in order to carry out differential image analysis using the differential in-gel analysis (DIA) and/or biological variation analysis (BVA) modules. Analysis by DIA was performed using default settings, and for each detection procedure the estimated number of spots was set to 3000. Differentially expressed proteins were evaluated by the average ratio, which represents the fold-change obtained comparing standardized abundance of the protein spots between two protein spot groups. A fold-change equal to twofold was set as the threshold to evaluate the differences in protein spot abundance. For BVA, statistical significance of differentially expressed proteins between normal mammary glands and mammary carcinomas was defined by the Student's *t*-test.

2.4 MS analysis

In order to identify the differentially abundant proteins, differential spots (or, for the isoelectric series, the three most abundant spots within the series) were excised, destained, trypsin digested overnight at 37°C (using 50–100 ng of trypsin, according to spot intensity), and subjected to LC-MS/MS analysis using one of the following platforms: (i) Q-TOF hybrid mass spectrometer equipped with a nano lock Z-spray source, and coupled on-line with a capillary chromatography system CapLC (Waters, Manchester, UK); (ii) XCT Ultra 6340 ion trap equipped with a 1200 HPLC system and a chip cube (Agilent Technologies, Palo Alto, CA, USA); (iii) LTQ Orbitrap Velos (Thermo Scientific, San Jose, CA, USA) interfaced with an UltiMate 3000 RSLCnano LC system (Dionex, Sunnyvale, CA, USA, now part of Thermo Scien-

tific). Generation and processing of Q-TOF (Waters) and XCT (Agilent) MS data were carried out according to previously reported protocols ([17] and [18], respectively). Concerning the LTQ-Orbitrap analyses, peptide mixtures were concentrated and desalted on a trapping precolumn (Acclaim PepMap C18, 75 μm × 2 cm nanoViper, 3 μm, 100 Å, Dionex), using 0.2% formic acid at a flow rate of 5 μL/min. The peptide separation was carried out at 35°C using a 75-μm id × 25 cm C18 column (Acclaim PepMap RSLC C18, 75 μm × 15 cm nanoViper, 2 μm, 100 Å, Dionex) at a flow rate of 300 nL/min, using a 25 min linear gradient from 1 to 50% eluent B (0.2% formic acid in 95% ACN) in eluent A (0.2% formic acid in 5% ACN). The mass spectrometer LTQ-Orbitrap Velos was set up in a data-dependent MS/MS mode under direct control of the Xcalibur software (version 1.0.2.65 SP2), where a full-scan spectrum (from 300 to 1700 *m/z*) was followed by tandem mass spectra (MS/MS). The instrument was operated in positive mode with a spray voltage of 1.2 kV, a capillary temperature of 275°C, and was calibrated before measurements. Full-scans were performed in the Orbitrap with resolution of 30 000 at 400 *m/z*, the automatic gain control was set to 1 000 000 ions and the lock mass option was enabled on a protonated polydimethylcyclsiloxane background ion ((Si(CH₃)₂O)₆; *m/z* = 445.120025) as internal recalibration for accurate mass measurements [19]. Peptide ions were selected as the ten most intense peaks (Top 10) of the previous scan. The signal threshold for triggering an MS/MS event was set to 500 counts. Higher energy collisional dissociation, performed at the far side of the C-trap, was chosen as the fragmentation method, by applying a 40% value for normalized collision energy, an isolation width of *m/z* 3.0, a Q-value of 0.25, and an activation time of 0.1 ms. Nitrogen was used as the collision gas. Precursor and fragment mass tolerance for protein identification were set to 10 ppm and 0.2 Da, respectively.

Proteome Discoverer platform (version 1.3; Thermo Scientific) interfaced with an in-house Mascot server (version 2.3, Matrix Science, London, UK) was used for protein identification, according to the following criteria: Database UniProtKB/Swiss-Prot (release 2012_03), Enzyme Trypsin, Maximum Missed Cleavage Sites 2, Taxonomy *Homo sapiens* (for human samples) or *mammalia* (for animal samples), cysteine carbamidomethylation as static modification, N-terminal glutamine conversion to pyro-glutamic acid, and methionine oxidation as dynamic modifications. Peptide Validator was used for peptide validation (peptide confidence: *p*-value < 0.01), and only rank 1 peptides were considered. Peptide and protein grouping were allowed, and strict maximum parsimony principle was applied.

3 Results

3.1 Human gastric adenocarcinoma

Tumor and normal adjacent tissue was collected from two cases of gastric adenocarcinoma archived as FFPE sample blocks in the Pathology Department of the CRO—National

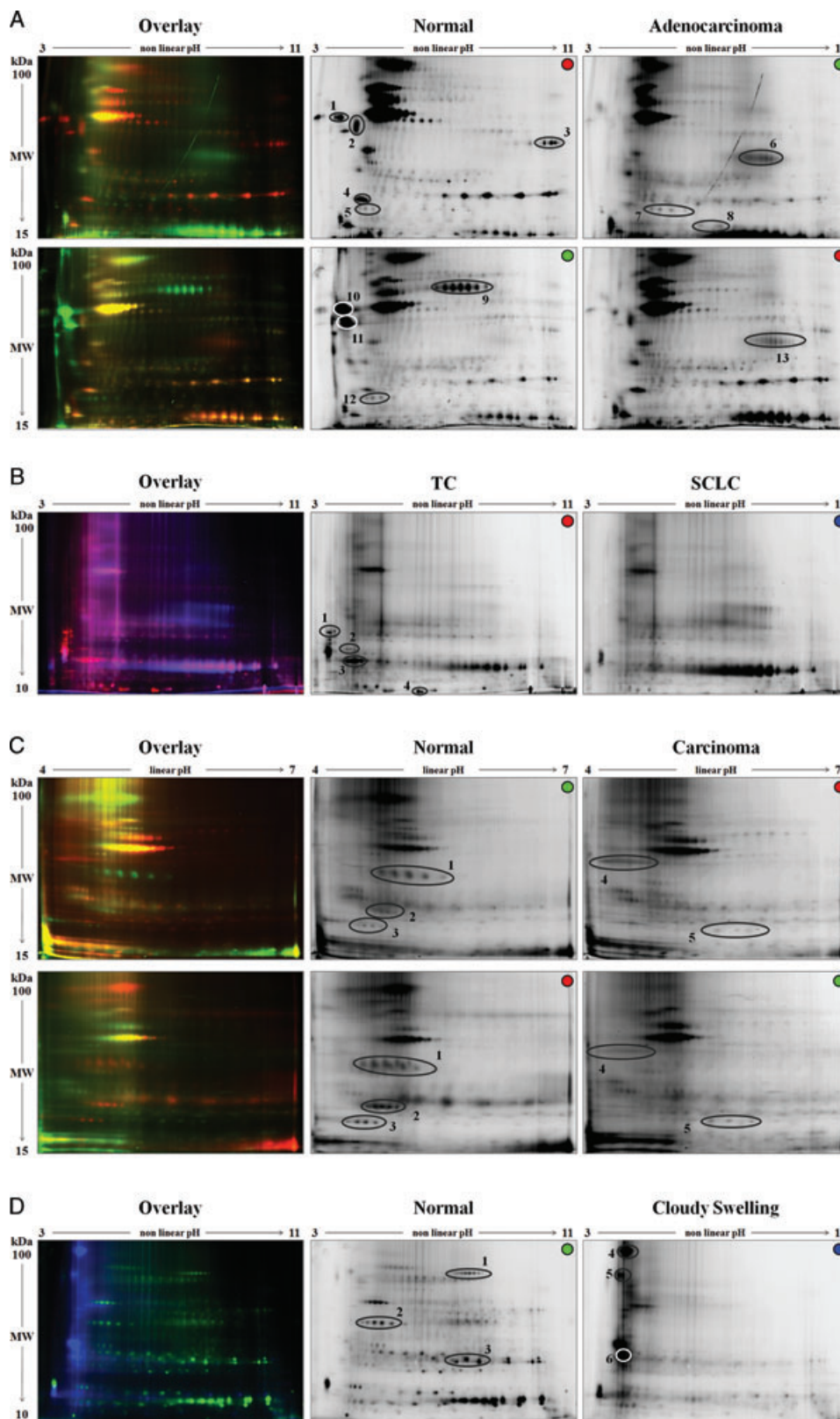


Figure 1. 2D-DIGE maps, including overlay (left) and single channel (center and right) images, obtained from human normal gastric tissue and gastric adenocarcinoma (A), human lung typical carcinoid (TC) and small cell lung carcinoma (SCLC) (B), canine normal mammary tissue and mammary tubulo-papillary carcinoma (C), and sheep liver tissue with normal histology and with signs of cloudy swelling and intracellular protein accumulation (D).

Cancer Institute (Aviano, Italy). Concerning the anatomical localization of the tissue fragments within the stomach, the first sample pair had been collected from the antrum, while the second from the fundus. The tissue sections were deparaffinized and subjected to protein extraction and cyanine labeling. Then, protein extracts obtained from tumor and normal tissue of each patient were run in a single DIGE gel, in order to carry out a separate DIA for each case by means of the DeCyder software. Overlay and single channel images of the 2D maps are shown in Fig. 1A. The number of spots detected in the 2D maps ranged from 378 to 596 (mean 463). Upon DIA analyses, eight and five spots (or spot clusters) showing differential abundance between tumor and normal in the first and second gel, respectively, were selected for MS analysis and protein identification. Differential spots are circled in Fig. 1A, and the corresponding protein identifications (as well as the average volume ratios related to DIA analysis) are listed in Table 3 (spot code A). Among differential proteins, several key digestive enzymes (pepsin A, gastricsin, also known as pepsinogen C, and gastric triacylglycerol lipase) were coherently found as massively underrepresented in the tumor tissue compared to the normal gastric mucosa. Moreover, gastrophilin-1 and calponin-1 were detected as underexpressed in gastric cancer; in both cases, an inverse correlation between protein expression and cancer development had been previously demonstrated [20,21]. On the other hand, nucleoside diphosphate kinase [22], stathmin [23], and peptidyl-prolyl *cis-trans* isomerase [24] have been associated in several studies to gastric cancer, or to malignant transformation in general.

3.2 Human lung neuroendocrine tumors

Two cases of lung neuroendocrine tumors (one typical carcinoid (TC) and one small cell lung carcinoma (SCLC)) archived as FFPE specimens in the Pathology Departments of the University of Verona and Sassari, respectively, were selected for the study. The tissue sections were deparaffinized and subjected to protein extraction and cyanine labeling. Then, the two protein extracts were run in a single DIGE gel, in order to carry out a DIA. Overlay and single channel images of the 2D maps are shown in Fig. 1B. The number of spots detected in the 2D maps were 335 (TC) and 281 (SCLC). Upon DIA analysis, four spots more abundant in the TC sample were selected for MS analysis and protein identification. Differential spots are circled in Fig. 1B, and the corresponding protein identifications (as well as the average volume ratios related to DIA analysis) are listed in Table 3 (spot code B). Chromogranin A and proSAAS were consistently related to the neuroendocrine differentiation of TC, as widely documented by the literature [25,26], whereas protein S100-A6 has been found in other studies as decreased in SCLC [27], or increased in endocrine tumors [28]. Interestingly, in these experiments, the 2D-DIGE technique revealed its unique ability to discriminate among different protein cleavage products, as opposed to shotgun

MS approaches. In fact, both chromogranin A and proSAAS are physiologically cleaved into various active (poly)peptides, three of which were clearly distinguishable in the 2D map. As shown in Fig. 2, spots B1 and B3 were both identified as chromogranin A, but the detected peptide sequences mapped to different regions of the protein (in the former case including pancreastatin, and in the latter corresponding to vasostatin-2) [29]. Concerning proSAAS, peptides identified within the spot B2 covered the central portion of the protein, while the active proSAAS-derived peptides were possibly cleaved, but obviously not visible on the 2D map because of their small size [30].

3.3 Canine mammary tumors

Four FFPE canine mammary tissue samples were collected from the repositories of the Veterinary Department at the University of Sassari. Among them, two were simple tubulopapillary mammary carcinomas and two were normal mammary glands. The tissue sections were deparaffinized and subjected to protein extraction and cyanine labeling; furthermore, an internal standard was prepared by equimolarly pooling the four sample protein extracts and labeled with the Cy2 fluorescent dye. Then, protein extracts were combined within two DIGE gels (4–7 pH range, one tumor and one control per gel, as detailed in Table 2) in order to carry out a BVA. Overlay and single channel images of the 2D maps are shown in Fig. 1C. The number of spots detected in the 2D maps ranged from 133 to 260 (mean 248). Upon BVA, five matched spots (or spot clusters) consistently showing differential abundance between tumor and normal (*t*-test *p*-value < 0.05) were selected for MS analysis and protein identification. Differential spots are circled in Fig. 1C, and the corresponding protein identifications (as well as the average volume ratios related to BVA) are listed in Table 3 (spot code C). Among differential proteins, myosin light chains were found as underexpressed in metastatic canine mammary carcinoma compared to nonmetastatic [31], whereas nucleophosmin and peroxiredoxin-6 were variously linked to breast cancer in earlier studies [32–35].

3.4 Heavy metal poisoning in sheep liver

Two liver tissue samples, one collected from a sheep affected by chronic liver degeneration and showing histological evidences of cloudy swelling and intracellular protein accumulation, and one collected from a healthy control, both archived as FFPE sample blocks in the Veterinary Department at the University of Sassari, were selected for the study. The samples had been collected from sheep grazing in an area subjected to exhaust fumes from a neighboring metallurgical industry, fixed, and archived as FFPE blocks. In the proteomics laboratory, the tissue sections were deparaffinized and subjected to protein extraction and cyanine labeling. Then, the

Table 3. List of MS identifications corresponding to differentially abundant spots

Spot code	DIGE average ratio	UniProt accession no.	Protein name	Calculated MW (kDa)	Calculated pI	Number of peptides	Number of PSMs	Sequence coverage (%)	MS instrument
Human gastric tissue (adenocarcinoma versus normal)									
A1	-15.83	P00790	Pepsin A	42	4.34	3	11	4.1	A
A2	-7.40	P20142	Gastricsin	42	4.46	2	10	5.2	W
A3	-22.54	P51911	Calponin-1	33	9.07	4	6	10.8	W
A4	-11.47	P24844	Myosin regulatory light polypeptide 9	20	4.92	6	7	33.7	W
A5	-3.01	Q9NS71	Gastrokine-1	22	6.32	4	6	19.1	A
A6	7.63	P68871	Hemoglobin subunit beta	16	7.28	9	15	68.7	A
		P02042	Hemoglobin subunit delta	16	8.05	9	13	73.5	A
		P69905	Hemoglobin subunit alpha	15	8.68	7	10	50.7	A
		P16152	Carbonyl reductase [NADPH] 1	30	8.32	5	6	30.3	A
A7	3.69	P15531	Nucleoside diphosphate kinase A	17	6.19	5	7	43.4	T
		P16949	Stathmin	17	5.97	5	6	25.5	T
A8	2.30	P62937	Peptidyl-prolyl <i>cis-trans</i> isomerase A	18	7.81	5	5	34.6	A
A9	-35.87	P07098	Gastric triacylglycerol lipase	45	7.33	6	7	13.8	W
A10 (= A1)	-37.51	P00790	Pepsin A	42	4.34	3	11	4.1	A
A11 (= A2)	-36.78	P20142	Gastricsin	42	4.46	2	10	5.2	W
A12 (= A5)	-7.29	Q9NS71	Gastrokine-1	22	6.32	4	6	19.1	A
A13 (= A6)	3.39	P68871	Hemoglobin subunit beta	16	7.28	9	15	68.7	A
		P02042	Hemoglobin subunit delta	16	8.05	9	13	73.5	A
		P69905	Hemoglobin subunit alpha	15	8.68	7	10	50.7	A
		P16152	Carbonyl reductase [NADPH] 1	30	8.32	5	6	30.3	A
Human lung neuroendocrine tumors (TC versus SCLC)									
B1	135.06	P10645	Chromogranin-A	51	4.60	3	4	15.1	W
B2	36.70	Q9UHG2	ProSAAS	27	6.62	5	5	25.8	W
B3	69.35	P10645	Chromogranin-A	51	4.60	4	12	15.1	W
B4	131.91	P06703	Protein S100-A6	10	5.48	2	2	16.7	W
Canine mammary tissue (tubulo-papillary carcinoma versus normal)									
C1	-9.27	P19006	Haptoglobin	36	6.09	6	15	21.9	T
C2	-9.33	A0JNJ5	Myosin light chain 1/3, skeletal muscle isoform	21	5.02	15	26	69.3	T
C3	-3.97	Q7M2V4	Myosin regulatory light chain 2, ventricular/ cardiac muscle isoform	19	5.00	14	16	66.7	T
C4	6.32	P06748	Nucleophosmin	33	4.78	10	24	32.7	T
C5	2.99	O08709	Peroxiredoxin-6	25	6.01	6	20	25.0	T
		Q6WIT9	Hypoxanthine-guanine phosphoribosyl-transferase	24	6.43	8	10	43.1	T
Sheep liver tissue (cloudy swelling versus normal)									
D1	-19.81	P00432	Catalase	60	7.28	10	18	26.6	W
D2	-2.66	Q9TTJ5	Regucalcin	33	5.77	5	6	20.7	W
D3	-7.26	O02691	3-hydroxyacyl-CoA dehydrogenase type-2	27	8.28	9	35	41.4	W
D4	29.82	P06761	78 kDa glucose-regulated protein	72	5.16	6	6	11.6	W
D5	7.02	P05307	Protein disulfide-isomerase	57	4.91	6	7	13.9	W
D6	6.96	Q32L47	ER resident protein 27	23	4.87	1	2	5.3	W

MS instrument: A, Agilent Chip Cube Ion Trap; T, Thermo LTQ-Orbitrap; W, Waters Q-TOF.

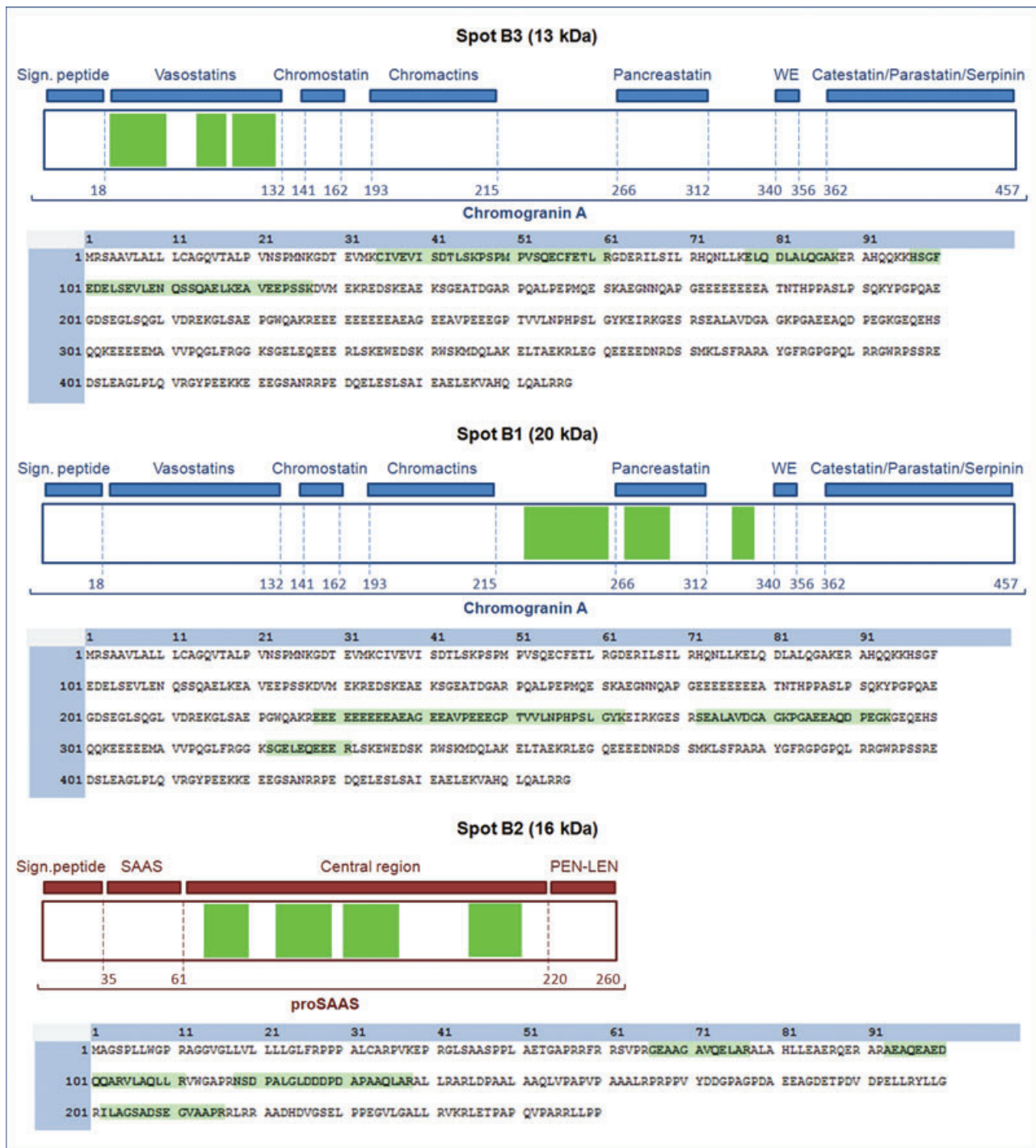


Figure 2. Schematic representation of the peptide sequences identified in three spots showing differential expression in typical carcinoid versus small cell lung carcinoma (TC versus SCLC, Fig. 1B). Cleavage sites and resulting peptides are illustrated on the parent proteins. The location of matched peptide sequences is indicated in green for each spot. Blue, chromogranin A; red, proSAAS.

two protein extracts were run in a single DIGE gel in order to carry out a DIA. Overlay and single channel images of the 2D maps are shown in Fig. 1D. The number of spots detected in the 2D maps were 482 (normal liver) and 308 (liver

with chronic degeneration). Upon DeCyder DIA, six spots (or spot clusters) showing differential abundance between the two samples were selected for MS analysis and protein identification. Differential spots are circled in Fig. 1D, and the

Clinical Relevance

Tissue biopsies collected from patients are fixed in formalin and embedded in paraffin to enable routine diagnostic procedures, whose results are then entered in the patients' clinical records. In the years, this has led to the generation of vast sample repositories with valuable associated retrospective information on diagnosis, prognosis, response to treatment, and outcome of the patient. Making these samples accessible to proteomic analysis can unleash a tremendous potential for our understanding of disease biology and for identification or validation of new

diagnostic and prognostic biomarkers. The ability to access the proteins trapped into these samples, with all their precious information, has spurred a significant wave of research studies aimed to provide methods for overcoming the fixation problem. Among other achievements, the potential applicability of 2D-PAGE and 2D-DIGE has been demonstrated on model tissues. This study was aimed to assess the potential of 2D-DIGE in providing meaningful information when applied to samples retrieved from different tissue repositories of human and veterinary hospitals.

corresponding protein identifications (as well as the average volume ratios related to DIA) are listed in Table 3 (spot code D). Among the proteins found as overexpressed in the intoxicated liver, 78 kDa glucose-regulated protein (GRP78), protein disulfide-isomerase, and ER resident protein 27 (ERp27) were of particular interest; in fact, these proteins have been reported as heavy metal intoxication markers or liver stress signal molecules [36–40] in other organisms, and their overexpression in sheep is strongly suggestive that the liver degeneration seen in these animals is most probably due to grazing in heavy metal contaminated pastures.

4 Discussion

The aim of the present study was to evaluate the applicability of 2D-DIGE to proteins extracted from a set of “real-world” FFPE tissues specimens collected from hospital archives. In fact, several sources of variability affect these samples, such as storage conditions before and after fixation, fixation times and protocols, tissue architectural features, block size, and others. Therefore, fixed human, dog and sheep tissues having different organ origin and disease traits were retrieved from four different biorepositories and subjected to full-length protein extraction, cyanine labeling, and 2D-DIGE analysis.

On the whole, the quality of the 2D proteome profile was similar to (or even better than) the previously published results obtained on model tissues [6–8]. However, as visually evident in Fig. 1, pattern complexity and S/N ratio varied slightly among samples, being surprisingly high in human gastric 2D maps and significantly lower (at least for basic, high-MW regions) for human lung and canine mammary samples. This may be due to differences in sample processing (for instance, in fixation time, as described in Table 1) as well as in the tissue composition and nature. Specifically, fixation time was found to considerably influence the quality of proteomic data in previous studies using MS-based approaches [41–43]; on the other hand, tissue-dependent variables are difficult to be controlled and measured.

A typical feature of FFPE protein extracts is the presence of artificial “protein complexes,” due to the residual protein–protein bonds caused by formaldehyde reactivity. An example of this phenomenon could be seen in spots A6 and A13, in which most of the identified peptides belong to hemoglobin subunits. Coherently, the apparent MW of both spots was approximately equal to that of a hemoglobin dimer (about 30 kDa). This supports the hypothesis that cross-links are likely to form in a stronger way among subunits of multimeric proteins because of their steric proximity, and therefore such subunits are difficult to be separated even using a combination of high temperature and high concentrations of detergents and reducing agents (as in the extraction procedure used in this work) [44].

The main result of this study is represented by the consistency in the identities of the differentially expressed proteins detected by MS with the biological and clinical features of the analyzed tissues. In fact, several known markers of gastric functionality, neuroendocrine differentiation, and malignant transformation were coherently detected in human gastric, human lung, and canine mammary tissue samples, respectively (Table 1).

Interestingly, several proteins found to be overexpressed in the sheep liver tissue with cloudy swelling and intracellular protein accumulation were consistent with a metal-induced, ER-related stress in liver, indicative of early cellular defense mechanisms. In fact, all the proteins showing differential expression levels in the affected sheep liver sample, such as GRP78, protein disulfide-isomerases, and ERp27, share functional properties and molecular pathways [45–47], and have been previously indicated as heavy metal intoxication markers [48–50] or liver stress signalers [51–53] in other organisms. The ability to apply 2D-DIGE to these archival samples highlighted the occurrence of these events also in the liver of sheep exposed to heavy metal intoxication by free grazing in areas exposed to industrial exhaust fumes.

These results point out that the information gathered by 2D-DIGE analysis of fixed tissues, although to a lower extent when compared to fresh samples, can be considered

as biologically meaningful and clinically applicable. In addition, the results shown highlighted an advantage of using a 2DE approach, that is, the visual detection of protein isoforms and/or cleavage products deriving from the same parent protein, and therefore of changes in their relative expression. As shown in Figs. 1B and 2, the 2D-DIGE approach enabled to discriminate two processed forms of chromogranin A, that is, vasostatin in a 13 kDa spot and a pancreastatin-containing domain in a 20 kDa spot (spots 3 and 1, respectively, Fig. 1B) [29]. In addition, proSAAS was identified in a 16 kDa spot, with peptides falling within the central region which results from processing of the N-terminal and C-terminal regions of the preprotein into bioactive peptides [30]. The detection of differences in expression of processed protein isoforms deriving from the same parent sequence, but having different molecular weights, can have very important biological consequences, especially in cases as this one, where a different neuroendocrine activity is dependent on such processing. The ability to apply 2D-DIGE to the full-length protein extracts generated from fixed tissues allowed the visualization of the differential abundance existing in these molecular weight products and their parent protein in the tissues under comparison. In fact, as opposed to shotgun proteomics, albeit generally recognized as being more sensitive and informative, the 2DE approach offers the significant advantage of enabling the detection of important differences in the MW and pI of full-length proteins that would generate virtually indistinguishable peptide sequences upon digestion, as it occurs during the shotgun proteomics procedure. In addition, the suitability of FFPE protein extracts to 2D-DIGE can provide a complementary approach to other gel-based and gel-free techniques in differential proteomic studies. In fact, it is now being increasingly demonstrated that quantitative proteomic information gained by means of different approaches, as robust and reliable as they can be individually, is typically more complete than the information gained by means of only one approach [54, 55]

In conclusion, this work contributes to prove the worth of 2D-DIGE in the field of clinical proteomics, specifically in studies based on the use of archival FFPE samples. In fact, 2D-DIGE can be fruitfully employed in differential proteomics studies involving archival specimens, at least as a complementary method, in view of its peculiarities enabling the immediate visual comparison of proteome patterns, as well as the direct visualization of spot shifts (due to PTMs or presence of protein isoforms) and of physiological/pathological protein cleavage products (as illustrated for neuroendocrine peptides). Last but not least, the results shown in this study add a further brick in the astoundingly growing building of FFPE proteomics, which holds promise of providing vast and robust clinical applications in the years to come.

This work was financed by Sardegna Ricerche—“Progetto Strategico Biotecnologie” programme. Dr. Tonina Roggio is acknowledged for her valuable support.

The authors have declared no conflict of interest.

5 References

- [1] Nirmalan, N. J., Harnden, P., Selby, P. J., Banks, R. E., Mining the archival formalin-fixed paraffin-embedded tissue proteome: opportunities and challenges. *Mol. Biosyst.* 2008, *4*, 712–720.
- [2] Blonder, J., Veenstra, T. D., Clinical proteomic applications of formalin-fixed paraffin-embedded tissues. *Clin. Lab. Med.* 2009, *29*, 101–113.
- [3] Tanca, A., Pagnozzi, D., Addis, M. F., Setting proteins free: progresses and achievements in proteomics of formalin-fixed, paraffin-embedded tissues. *Proteomics Clin. Appl.* 2012, *6*, 7–21.
- [4] Magdeldin, S., Yamamoto, T., Toward deciphering proteomes of formalin-fixed paraffin-embedded (FFPE) tissues. *Proteomics* 2012, *12*, 1045–1058.
- [5] Ralton, L. D., Murray, G. I., The use of formalin fixed wax embedded tissue for proteomic analysis. *J. Clin. Pathol.* 2011, *64*, 297–302.
- [6] Addis, M. F., Tanca, A., Pagnozzi, D., Rocca, S. et al., 2-D PAGE and MS analysis of proteins from formalin-fixed, paraffin-embedded tissues. *Proteomics* 2009, *9*, 4329–4339.
- [7] Azimzadeh, O., Barjaktarovic, Z., Aubele, M., Calzada-Wack, J. et al., Formalin-fixed paraffin-embedded (FFPE) proteome analysis using gel-free and gel-based proteomics. *J. Proteome Res.* 2010, *9*, 4710–4720.
- [8] Tanca, A., Pagnozzi, D., Falchi, G., Tonelli, R. et al., Application of 2-D DIGE to formalin-fixed, paraffin-embedded tissues. *Proteomics* 2011, *11*, 1005–1011.
- [9] Shi, S., Key, M., Kalra, K., Antigen retrieval in formalin-fixed, paraffin-embedded tissues: an enhancement method for immunohistochemical staining based on microwave oven heating of tissue sections. *J. Histochem. Cytochem.* 1991, *39*, 741–748.
- [10] Shi, S. R., Shi, Y., Taylor, C. R., Antigen retrieval immunohistochemistry: review and future prospects in research and diagnosis over two decades. *J. Histochem. Cytochem.* 2011, *59*, 13–32.
- [11] Celis, J. E., Gel-based proteomics: what does MCP expect? *Mol. Cell. Proteomics* 2004, *3*, 949.
- [12] Chevalier, F., Highlights on the capacities of “Gel-based” proteomics. *Proteome Sci.* 2010, *8*, 23.
- [13] Unlu, M., Morgan, M. E., Minden, J. S., Difference gel electrophoresis: a single gel method for detecting changes in protein extracts. *Electrophoresis* 1997, *18*, 2071–2077.
- [14] Lilley, K. S., Friedman, D. B., All about DIGE: quantification technology for differential-display 2D-gel proteomics. *Expert Rev. Proteomics* 2004, *1*, 401–409.
- [15] Viswanathan, S., Unlu, M., Minden, J. S., Two-dimensional difference gel electrophoresis. *Nat. Protoc.* 2006, *1*, 1351–1358.

- [16] Addis, M. F., Tanca, A., Pagnozzi, D., Crobu, S. et al., Generation of high-quality protein extracts from formalin-fixed, paraffin-embedded tissues. *Proteomics* 2009, 9, 3815–3823.
- [17] Pisanu, S., Ghisaura, S., Pagnozzi, D., Biosa, G. et al., The sheep milk fat globule membrane proteome. *J. Proteomics* 2011, 74, 350–358.
- [18] Biosa, G., Addis, M. F., Tanca, A., Pisanu, S. et al., Comparison of blood serum peptide enrichment methods by Tricine SDS-PAGE and mass spectrometry. *J. Proteomics* 2011, 75, 93–99.
- [19] Olsen, J. V., de Godoy, L. M., Li, G., Macek, B. et al., Parts per million mass accuracy on an Orbitrap mass spectrometer via lock mass injection into a C-trap. *Mol. Cell. Proteomics* 2005, 4, 2010–2021.
- [20] Oien, K. A., McGregor, F., Butler, S., Ferrier, R. K. et al., Gastrin 1 is abundantly and specifically expressed in superficial gastric epithelium, down-regulated in gastric carcinoma, and shows high evolutionary conservation. *J. Pathol.* 2004, 203, 789–797.
- [21] Taniguchi, S., Suppression of cancer phenotypes through a multifunctional actin-binding protein, calponin, that attacks cancer cells and simultaneously protects the host from invasion. *Cancer Sci.* 2005, 96, 738–746.
- [22] Tee, Y. T., Chen, G. D., Lin, L. Y., Ko, J. L. et al., Nm23-H1: a metastasis-associated gene. *Taiwan J. Obstet. Gynecol.* 2006, 45, 107–113.
- [23] Jeon, T. Y., Han, M. E., Lee, Y. W., Lee, Y. S. et al., Overexpression of stathmin1 in the diffuse type of gastric cancer and its roles in proliferation and migration of gastric cancer cells. *Br. J. Cancer* 2010, 102, 710–718.
- [24] Gong, Y. H., Chen, M., Xu, Y., Dong, N. et al., Subtractive hybridization analysis of gastric diseases-associated *Helicobacter pylori* identifies peptidyl-prolyl isomerase as a potential marker for gastric cancer. *FEMS Microbiol. Lett.* 2011, 320, 103–109.
- [25] Rekhman, N., Neuroendocrine tumors of the lung: an update. *Arch. Pathol. Lab. Med.* 2010, 134, 1628–1638.
- [26] Fricker, L. D., McKinzie, A. A., Sun, J., Curran, E. et al., Identification and characterization of proSAAS, a granin-like neuroendocrine peptide precursor that inhibits prohormone processing. *J. Neurosci.* 2000, 20, 639–648.
- [27] Lee, H. S., Park, J. W., Chertov, O., Colantonio, S. et al., Matrix-assisted laser desorption/ionization mass spectrometry reveals decreased calyculin expression in small cell lung cancer. *Pathol. Int.* 2012, 62, 28–35.
- [28] Sofiadis, A., Dinets, A., Orre, L. M., Branca, R. M. et al., Proteomic study of thyroid tumors reveals frequent up-regulation of the Ca²⁺-binding protein S100A6 in papillary thyroid carcinoma. *Thyroid* 2010, 20, 1067–1076.
- [29] Koshimizu, H., Kim, T., Cawley, N. X., Loh, Y. P., Chromogranin A: a new proposal for trafficking, processing and induction of granule biogenesis. *Regul. Pept.* 2010, 160, 153–159.
- [30] Wardman, J. H., Berezniuk, I., Di, S., Tasker, J. G. et al., ProSAAS-derived peptides are colocalized with neuropeptide Y and function as neuropeptides in the regulation of food intake. *PLoS ONE* 2011, 6, e28152.
- [31] Klopffleisch, R., Klose, P., Weise, C., Bondzio, A. et al., Proteome of metastatic canine mammary carcinomas: similarities to and differences from human breast cancer. *J. Proteome Res.* 2010, 9, 6380–6391.
- [32] Rower, C., Ziems, B., Radtke, A., Schmitt, O. et al., Toponostics of invasive ductal breast carcinoma: combination of spatial protein expression imaging and quantitative proteome signature analysis. *Int. J. Clin. Exp. Pathol.* 2011, 4, 454–467.
- [33] Rower, C., Koy, C., Hecker, M., Reimer, T. et al., Mass spectrometric characterization of protein structure details refines the proteome signature for invasive ductal breast carcinoma. *J. Am. Soc. Mass Spectrom.* 2011, 22, 440–456.
- [34] Chang, X. Z., Li, D. Q., Hou, Y. F., Wu, J. et al., Identification of the functional role of peroxiredoxin 6 in the progression of breast cancer. *Breast Cancer Res.* 2007, 9, R76.
- [35] Goncalves, K., Sullivan, K., Phelan, S., Differential expression and function of peroxiredoxin 1 and peroxiredoxin 6 in cancerous MCF-7 and noncancerous MCF-10A breast epithelial cells. *Cancer Invest.* 2012, 30, 38–47.
- [36] Alanen, H. I., Williamson, R. A., Howard, M. J., Hatahet, F. S. et al., ERp27, a new non-catalytic endoplasmic reticulum-located human protein disulfide isomerase family member, interacts with ERp57. *J. Biol. Chem.* 2006, 281, 33727–33738.
- [37] Wong, L. L., Fan, S. T., Man, K., Sit, W. H. et al., Identification of liver proteins and their roles associated with carbon tetrachloride-induced hepatotoxicity. *Hum. Exp. Toxicol.* 2011, 30, 1369–1381.
- [38] Shinkai, Y., Yamamoto, C., Kaji, T., Lead induces the expression of endoplasmic reticulum chaperones GRP78 and GRP94 in vascular endothelial cells via the JNK-AP-1 pathway. *Toxicol. Sci.* 2010, 114, 378–386.
- [39] Lou, L. X., Geng, B., Chen, Y., Yu, F. et al., Endoplasmic reticulum stress involved in heart and liver injury in iron-loaded rats. *Clin. Exp. Pharmacol. Physiol.* 2009, 36, 612–618.
- [40] Liu, F., Inageda, K., Nishitai, G., Matsuoka, M., Cadmium induces the expression of Grp78, an endoplasmic reticulum molecular chaperone, in LLC-PK1 renal epithelial cells. *Environ. Health Perspect.* 2006, 114, 859–864.
- [41] Sprung, R. W., Brock, J. W. C., Tanksley, J. P., Li, M. et al., Equivalence of protein inventories obtained from formalin-fixed paraffin-embedded and frozen tissue in multidimensional liquid chromatography-tandem mass spectrometry shotgun proteomic analysis. *Mol. Cell. Proteomics* 2009, 8, 1988–1998.
- [42] Wolff, C., Schott, C., Porschewski, P., Reischauer, B. et al., Successful protein extraction from over-fixed and long-term stored formalin-fixed tissues. *PLoS ONE* 2011, 6, e16353.
- [43] Tanca, A., Pagnozzi, D., Falchi, G., Biosa, G. et al., Impact of fixation time on GeLC-MS/MS proteomic profiling of formalin-fixed, paraffin-embedded tissues. *J. Proteomics* 2011, 74, 1015–1021.
- [44] Nirmalan, N. J., Harnden, P., Selby, P. J., Banks, R. E., Development and validation of a novel protein extraction methodology for quantitation of protein expression in formalin-fixed paraffin-embedded tissues using western blotting. *J. Pathol.* 2009, 217, 497–506.

- [45] Rabek, J. P., Boylston, W. H., 3rd, Papaconstantinou, J., Carbonylation of ER chaperone proteins in aged mouse liver. *Biochem. Biophys. Res. Commun.* 2003, *305*, 566–572.
- [46] Song, J., Finnerty, C. C., Herndon, D. N., Boehning, D. et al., Severe burn-induced endoplasmic reticulum stress and hepatic damage in mice. *Mol. Med.* 2009, *15*, 316–320.
- [47] Alanen, H. I., Williamson, R. A., Howard, M. J., Hatahet, F. S. et al., ERp27, a new non-catalytic endoplasmic reticulum-located human protein disulfide isomerase family member, interacts with ERp57. *J. Biol. Chem.* 2006, *281*, 33727–33738.
- [48] Liu, F., Inageda, K., Nishitai, G., Matsuoka, M., Cadmium induces the expression of Grp78, an endoplasmic reticulum molecular chaperone, in LLC-PK1 renal epithelial cells. *Environ. Health Perspect.* 2006, *114*, 859–864.
- [49] Lou, L. X., Geng, B., Chen, Y., Yu, F. et al., Endoplasmic reticulum stress involved in heart and liver injury in iron-loaded rats. *Clin. Exp. Pharmacol. Physiol.* 2009, *36*, 612–618.
- [50] Qian, Y., Zheng, Y., Ramos, K. S., Tiffany-Castiglioni, E., GRP78 compartmentalized redistribution in Pb-treated glia: role of GRP78 in lead-induced oxidative stress. *Neurotoxicology* 2005, *26*, 267–275.
- [51] Morrison, D. K., The 14-3-3 proteins: integrators of diverse signalling cues that impact cell fate and cancer development. *Trends Cell. Biol.* 2009, *19*, 16–23.
- [52] Lee, I. N., Chen, C. H., Sheu, J. C., Lee, H. S. et al., Identification of human hepatocellular carcinoma-related biomarkers by two-dimensional difference gel electrophoresis and mass spectrometry. *J. Proteome Res.* 2005, *4*, 2062–2069.
- [53] Grune, T., Reinheckel, T., Li, R., North, J. A. et al., Proteasome-dependent turnover of protein disulfide isomerase in oxidatively stressed cells. *Arch. Biochem. Biophys.* 2002, *397*, 407–413.
- [54] Wu, W. W., Wang, G., Baek, S. J., Shen R. F., Comparative study of three proteomic quantitative methods, DIGE, cIAT, and iTRAQ, using 2D Gel- or LC-MALDI TOF/TOF. *J. Proteome Res.* 2006, *5*, 651–658.
- [55] Piersma, S. R., Fiedler, U., Span, S., Lingnau, A. et al., Workflow comparison for label-free, quantitative secretome proteomics for cancer biomarker discovery: method evaluation, differential analysis, and verification in serum. *J. Proteome Res.* 2010, *9*, 1913–1922.